Fracture 1977, Volume 2, ICF4, Waterloo, Canada, June 19 - 24, 1977

CORRELATIONS BETWEEN FRACTURE TOUGHNESS, TENSILE PROPERTIES, FRACTURE MORPHOLOGY, AND MICROSTRUCTURE OF A HIGH-STRENGTH STEEL

K-H. Schwalbe* and W. Backfisch**

INTRODUCTION

Comprehensive research has demonstrated that fracture toughness is a complex mechanical property being related to a number of "basic mechanical properties", such as elastic properties (modulus of elasticity), plastic properties (yield strength, strain hardening), ductility, and microstructure. Generally, K_{Ic} is determined by a combination of these properties although it is often possible to regard K_{Ic} as a function of a single of these properties.

In the work described in the present paper the behaviour of cracks in a high-strength, low-alloy steel was investigated by measurement and observation of plane strain fracture toughness, tensile properties, fracture surface appearance, and microstructure. The information thereby obtained was used to verify a K_{Ic}-calculation model.

EXPERIMENTAL

The composition of the steel investigated is given in Table 1.

Plane strain fracture toughness was measured on three point bend specimens (20 x 40 x 160 mm) according to the ASTM test procedure. The specimens were austenitized at 850°C and oil quenched to room temperature and tempered at 100, 200, 300, 400, 500 and 600°C. From the broken bend specimens round tensile specimens and plane strain tensile specimens were machined which were then used to measure the 0.2% offset yield strength, σ_y, the strain hardening exponent, n, and the true fracture strain

$$\varepsilon_f = \ln \frac{A_o}{A_f} \qquad (1)$$

The fracture surfaces of the bend specimens were examined in a scanning electron microscope (SEM). Transmission electron microscopy (TEM), light microscopy and SEM were used to reveal the microstructure. In addition, replicas of the fracture surfaces were examined in the TEM.

RESULTS AND DISCUSSION

Figure 1 shows fracture toughness, yield strength and strain hardening exponent (both measured on round tensile specimens), and true fracture

*DFVLR, (German Aerospace Research Establishment), 5000 Koeln 90, Linder Hoehe, West-Germany.
**Institut fuer Werkstoffkunde I, Universitaet Karlsruhe, 7500 Karlsruhe, Kaiserstrasse 12, West-Germany.

strain (measured on plane strain tensile specimens) as a function of the tempering temperature.

Figures 2 and 3 show micrographs of the microstructures obtained at 200 and 600°C. At 200°C the microstructure consists of martensite plates with fine precipitates. The martensite plates are approximately 0.5 μm thick and 3 to 6 μm in diameter. The transformation of martensite with increasing tempering temperature leads to a microstructure consisting of ferrite plus cementite. According to the TEM micrographs cementite precipitates in the form of stringers of elongated particles which seem to be located at the former martensite plate boundaries. Comparing the micrographs of different tempering treatments it is seen that some particles grow in size at the expense of others giving rise to increasing fragmentation of the stringers with increasing tempering temperature. The dark lines marking the martensite plate boundaries at 200°C may be indicative of an early stage of cementite precipitation. By this transformation mechanism the martensite plate pattern is preserved up to 600°C. Precipitation also takes place in the interior of the plates but by smaller particles than at the plate boundaries.

The fracture surface observations reveal dimple structure throughout the entire tempering temperature range. An example is shown in Figure 4. Thus, the K_{Ic} minimum at 300°C cannot be explained by low energy crack propagation along prior austenite grain boundaries as in other cases [1]. Average values for the microstructural element size, d* (by "microstructural element" the martensite and ferrite plates, respectively, are meant) and the dimple diameter were determined and plotted in Figure 5 versus tempering temperature. The close coincidence between the two curves suggests that on the average one dimple is formed in one microstructural element. A similar result has also been obtained on Ti6Al4V [2] where the grain size corresponded to the dimple size. A closer examination of the fracture surfaces reveals two characteristic dimple sizes, namely approximately 0.5 μm and 5 μm. Comparing these numbers with thickness and width of the martensite and ferrite plates it is tentatively suggested that the plates are mainly cut either in their thickness direction or parallel to their symmetry plane. Further experiments are planned to clarify this assumption. In Figure 6 a possible crack propagation mechanism for these two cases is drawn schematically. Voids are formed at cementite particles and are linked up by plastic deformation of the matrix. In case of crack propagation perpendicular to the plates, the resulting dimple size corresponds to the plate thickness, Figure 6a. In case of crack propagation parallel to a plate, several voids may be nucleated and linked up to a large shallow dimple, Figure 6b.

Looking at the planar array of the hard cementite particles, one should expect relatively brittle crack propagation along the cementite stringers since such networks of brittle phases represent a low energy crack path [3]. But actually, the material behaves in a ductile manner. Two reasons may account for that:

a) Crack propagation along the plate boundaries would imply frequent crack path deviation, increase of the real fracture surface, and hence increase of the crack propagation resistance. From titanium alloys it is known that this effect occurs in the Widmannstatten microstructure which is geometrically comparable to the microstructure of the present material.

b) Brittle crack propagation along weak planes would require high local normal stresses. But due to the small "grain size" of the microstructure only short slip planes and correspondingly short dislocation pile-ups can occur. If the brittle particles would be located at the prior austenite grain boundaries the active grain size (austenite grain size) and hence the probability for large pile-ups and normal stress controlled brittle crack propagation would be much larger. In fact, embrittling is observed when a carbide film [3] or impurity segregation are located at prior austenite grain boundaries [1].

K_{Ic} CALCULATION MODEL

According to Krafft's model [4] instability occurs when a critical strain occurs over the process zone size. The process zone size is the smallest material dimension necessary for the formation of a crack propagation element, i.e. one dimple. In terms of the microstructure, the process zone size corresponds to the inclusion distance if inclusions are the void nucleating sites. In the present case the microstructural element size, d*, is the relevant quantity.

Concerning the critical strain, it is assumed that the logarithmic fracture strain (equation (1)) measured on plane strain tensile specimens represents a reasonable measure.

As there exists no closed-form solution for the strain distribution in a crack opening mode I plastic zone a strain distribution in analogy to mode III is assumed [5]

$$\varepsilon = \varepsilon_y \left[\frac{\omega}{x}\right]^{1/1+n} \tag{2}$$

where

$$\omega = (1-2\nu)\ \frac{K^2}{(1+n)\ \pi\ \sigma_y^{\ 2}} \tag{3}$$

ε_y: yield strain, n: strain hardening exponent and x: distance from crack tip.

Setting $\varepsilon = \varepsilon_f$ and $x = d^*$ equation (2) yields

$$K = K_{Ic} = \frac{\sigma_y}{1-2\nu}\sqrt{\pi\ (1+n)\, d^* \left[\frac{\varepsilon_f\ E}{\sigma_y}\right]^{1+n}} \tag{4}$$

This equation relates tensile properties and a microstructural parameter to fracture toughness. By definition, K_{Ic} is considered to be that stress intensity that causes a crack growth increment equal to the dimple size. In Figure 7 the calculated values are plotted along with the experimental values. In spite of the simplicity of the calculation model it yields realistic results. Again, it can be stated that fracture toughness is not a function of a single other material property. Rather, it is the result of the combined action of a number of material properties. Equation (4) may give an impression of the way by which these properties affect K_{Ic}.

REFERENCES

1. ZACKAY, V. F., 40th Meeting of the AGARD Structure and Materials Panel, Brussels, Belgium, 1975.
2. GALDA, K. H., MUNZ, D. and SCHWALBE, K-H., 3rd International Conference on Titanium, Moscow, 1976.
3. WEI, R. P., in ASTM STP 381, 1965.
4. KRAFFT, J. M., Appl. Mat. Res. 3, 1964, 88.
5. SCHWALBE, K-H, Eng. Fracture Mech. 6, 1974, 415.

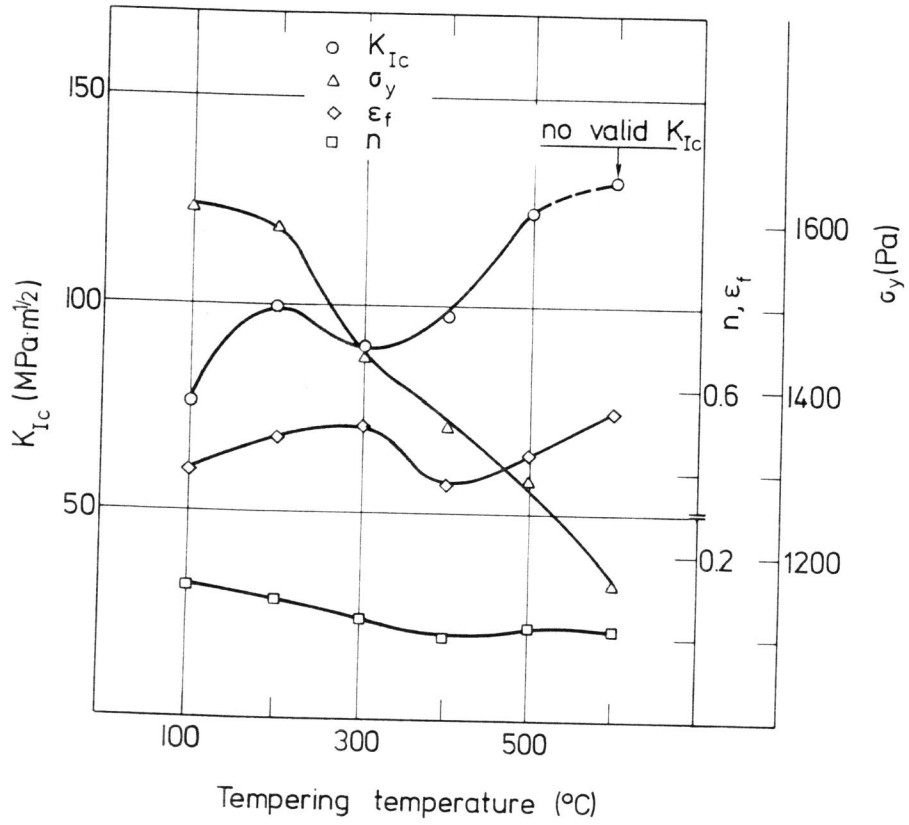

Figure 1 Mechanical Properties vs. Tempering Temperature

Figure 2 Microstructure after 200° C Temper.

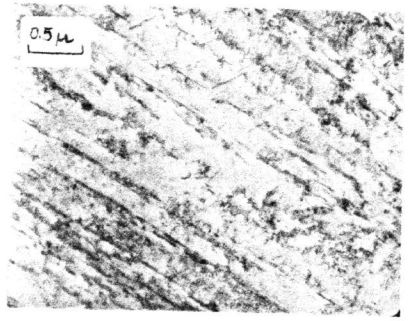

Figure 3 Microstructure after 600° Temper

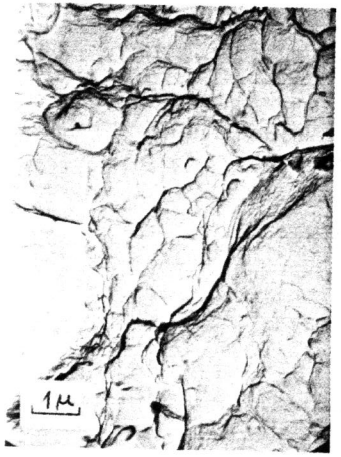

Figure 4 Fracture Surface after 300° C Temper, Replica

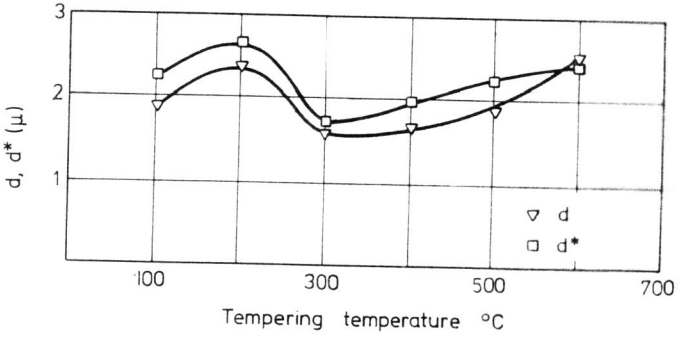

Figure 5 Average Dimple Diameter, d, and Microstructural Element Size, d*, vs. Tempering Temperature

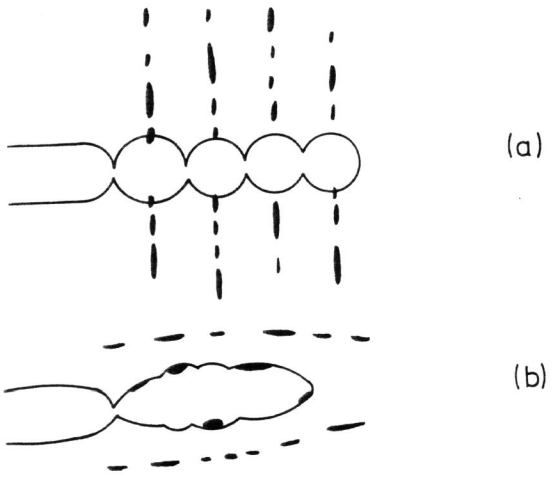

Figure 6 Crack Propagation, (a) Perpendicular, (b) Parallel to the Microstructural Plates

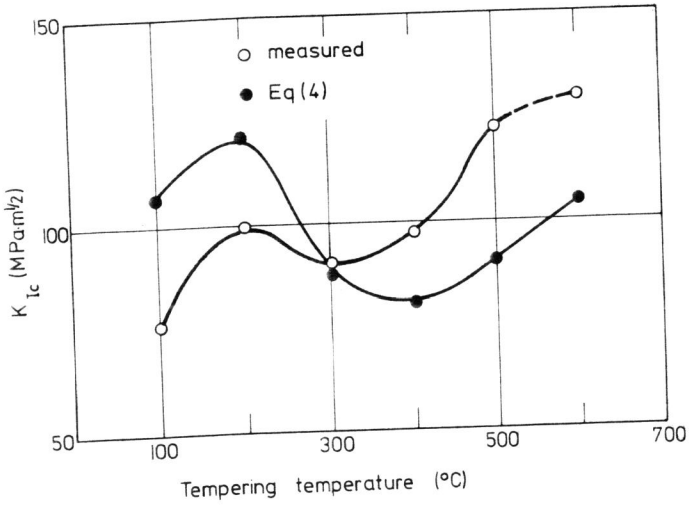

Figure 7 Measured and Calculated K_{Ic} Values

Table 1

Composition in weight %							
C	Si	Mn	P	S	Cr	Ni	Mo
0.35	0.27	0.63	0.007	0.006	1.30	3.30	0.47